



Viburnum opulus fruit extract-capped gold nanoparticles attenuated oxidative stress and acute inflammation in carrageenan-induced paw edema model

Cristina Bidian, Gabriela Adriana Filip, Luminița David, Bianca Moldovan, Ioana Baldea, Diana Olteanu, Mara Filip, Pompei Bolfa, Monica Potara, Alina Mihaela Toader & Simona Clichici

To cite this article: Cristina Bidian, Gabriela Adriana Filip, Luminița David, Bianca Moldovan, Ioana Baldea, Diana Olteanu, Mara Filip, Pompei Bolfa, Monica Potara, Alina Mihaela Toader & Simona Clichici (2022) *Viburnum opulus* fruit extract-capped gold nanoparticles attenuated oxidative stress and acute inflammation in carrageenan-induced paw edema model, Green Chemistry Letters and Reviews, 15:2, 320-336, DOI: [10.1080/17518253.2022.2061872](https://doi.org/10.1080/17518253.2022.2061872)

To link to this article: <https://doi.org/10.1080/17518253.2022.2061872>



© 2022 The Author(s). Published by Informa UK Limited, trading as Taylor & Francis Group



Published online: 12 Apr 2022.



[Submit your article to this journal](#)



Article views: 1842



[View related articles](#)



[View Crossmark data](#)



Citing articles: 1 [View citing articles](#)

RESEARCH ARTICLE

 OPEN ACCESS  Check for updates

Viburnum opulus fruit extract-capped gold nanoparticles attenuated oxidative stress and acute inflammation in carrageenan-induced paw edema model

Cristina Bidian^a, Gabriela Adriana Filip^a, Luminița David^b, Bianca Moldovan^b, Ioana Baldea^a, Diana Olteanu^a, Mara Filip^a, Pompei Bolfa^{c,d}, Monica Potara^e, Alina Mihaela Toader^a and Simona Clichici^a

^aDepartment of Physiology, 'Iuliu Hatieganu' University of Medicine and Pharmacy, Cluj-Napoca, Romania; ^bDepartment of Chemistry, Faculty of Chemistry and Chemical Engineering, 'Babes-Bolyai' University, Cluj-Napoca, Romania; ^cDepartment of Pathology, University of Agricultural Sciences and Veterinary Medicine, Cluj-Napoca, Romania; ^dDepartment of Biomedical Sciences, Ross University School of Veterinary Medicine, Basseterre, West Indies; ^eNanobiophotonics and Laser Microspectroscopy Center, Interdisciplinary Research Institute in Bio-Nano-Sciences, Babes-Bolyai University, Cluj-Napoca, Romania

ABSTRACT

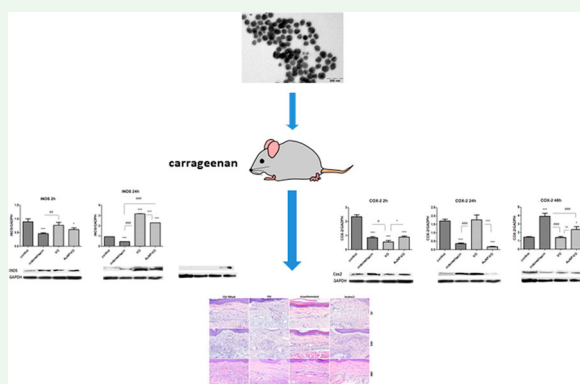
This study designed, characterized, and investigated the antioxidant and anti-inflammatory effects of gold nanoparticles coated with *Viburnum opulus* extract (AuNP-VO) compared to those of *Viburnum opulus* fruit extract (VO) and indomethacin, on experimental inflammation in Wistar rats. The structure and properties of the synthesized AuNPs-VO were evaluated by UV-Vis spectroscopy, transmission electron microscopy (TEM), dynamic light scattering (DLS), and zeta potential measurements. Their biological effects on paw inflammation were assessed at 2, 24, and 48 h after the administration of plantar carrageenan by quantifying oxidative stress and inflammation and by histopathological analysis. TEM micrographs confirmed the spherical shape, homogeneous distribution, and nano-size of 65 nm. AuNP-VO and VO showed antioxidant and anti-inflammatory effects on plantar inflammation with different dynamics of action. AuNP-VO exerted antioxidant effects, especially, at 48 h and diminished the plantar inflammation in the early stages (IL-1 α , IL-1 β , IL-6, TNF- α and IL-10) and late stages (IL-1 β , $p < 0.01$) whereas VO reduced the inflammatory response, predominantly in the early stages ($p < 0.01$; $p < 0.001$), and maintained reduced IL-1 β values ($p < 0.001$) and a lower histopathological inflammatory score at 48 h. In conclusion, AuNP-VO and VO extract can be used as valuable agents for the treatment of diseases associated with inflammation.

ARTICLE HISTORY

Received 28 February 2022
Accepted 31 March 2022

KEYWORDS

Gold nanoparticles;
Viburnum opulus; oxidative stress; inflammation



Introduction

Inflammation is a complex biological phenomenon that plays a protective role in maintaining the integrity of the body against physical, chemical, or infectious agents. Numerous studies have shown that inflammation has been involved in the pathogenesis of different diseases (1) such as: diabetes (2),

obstructive pulmonary disease (3), asthma (4), arthritis (5), infectious diseases (6) and malignant tumors (7).

In inflammation, polymorphonuclear neutrophils (PMNs) play an important role because of their migration in inflamed tissues, attraction to chemokines, and due to their ability to eliminate pathogens by degranulation,

CONTACT Gabriela Adriana Filip  adrianafilip33@yahoo.com  Department of Physiology, "Iuliu Hatieganu" University of Medicine and Pharmacy, 1-3 Clinicilor Street, Cluj-Napoca 400006, Romania

© 2022 The Author(s). Published by Informa UK Limited, trading as Taylor & Francis Group

This is an Open Access article distributed under the terms of the Creative Commons Attribution License (<http://creativecommons.org/licenses/by/4.0/>), which permits unrestricted use, distribution, and reproduction in any medium, provided the original work is properly cited.

phagocytosis, neutrophil extracellular traps, and cytokine release (8). Endogenous reactive oxygen species (ROS), released by NADPH-oxidase activity regulate pathways dependent on tyrosine phosphorylation, control phagocytosis, and modulate the expression of cytokines and chemokines involved in the inflammatory response (9).

The key mediator of inflammation is the nuclear transcription factor (NF)- κ B. This factor, after activation by oxidizing factors, lipid mediators, bacterial products, cytokines, and viral proteins, amplifies the inflammatory response by overregulating inflammatory mediators including cyclooxygenase-2 (COX-2), inflammatory cytokines, and inducible nitric oxide synthase (iNOS).

Proinflammatory cytokines are immunoregulatory mediators secreted by immune cells (macrophages and monocytes) and non-immune cells (fibroblasts and endothelial cells) in response to various stimuli (10). TNF- α and IL-1 β stimulate PGE₂ formation after COX-2 activation. In addition, TNF- α triggers iNOS expression, increases neutrophil migration (11) and initiates nitric oxide (NO) synthesis. The constitutive isoforms, neuronal NOS (nNOS) and endothelial NOS (eNOS), produce small amounts of NO, which acts as a neurotransmitter and vasodilator. Inducible isoform (iNOS) generates large amounts of NO, especially during inflammatory reactions (12–14). At high concentrations, NO reacts with superoxide anions to form peroxynitrite, which is responsible for oxidative stress and inflammatory cellular changes (15). To counteract the inflammation, the anti-inflammatory cytokines such as IL-10, IL-11, IL-13, IL-4 and IL-5 are secreted (16, 17).

Conventional therapies used in inflammation are mainly non-steroidal anti-inflammatory drugs, which are very effective agents but have many side effects. Because oxidative mechanisms are at the origin of inflammation, it has been suggested that antioxidants have anti-inflammatory effects and no side effects. In this context, natural compounds from plants and fruits have been increasingly used in medical practice as adjuvants for inflammatory conditions.

Viburnum opulus (VO) belongs to the genus *Viburnum* and family *Aldoxaceae*. The fruits have antioxidant properties due to their high content of anthocyanins, flavonoids, phenolic acids, tannins, and vitamins (18, 19). Antioxidant ability has been demonstrated *in vitro* in human cell cultures (Caco-2 adenocarcinoma, SH-SY5Y neuronal cells) (19, 20) and mouse cells (MIN-6 insuloma, 3T3 adipocytes -L1) (21, 22).

The rapid development of nanotechnology in recent years has made nanoparticles ubiquitous. There is a wide range of metal nanoparticles, made of various materials, having different shapes and sizes (23, 24, 25,

26). Gold nanoparticles are frequently used in medicine for diagnostic or therapeutic purposes, for the administration of drugs or as new therapeutic agents, in the treatment of some forms of cancer: lung cancer (27, 28), colorectal cancer (27, 29), breast cancer (30, 31), cervical cancer (32, 33), leukaemia (34).

Nanoparticles reach the body in different ways: oral, injectable, inhaler or transdermal. Their absorption and solubility depend on their size, surface charge, concentration, and pH (35). They enter the circulatory system and interact with blood plasma proteins, which form a protein crown around nanoparticles. Immunoglobulins G, M, and fibrinogen have been detected in almost all nanoparticles (36).

Gold nanoparticles (AuNPs) exert immunomodulatory effects by inhibiting nuclear factor kappa B (NF- κ B) expression; consequently, they decrease COX-2 and iNOS expression and proinflammatory cytokine production (37).

AuNPs have been shown to selectively inhibit the production of IL-1 β , IL-17, and TNF- α , decrease IL-12, and alter the cellular immune response from TH1 (proinflammatory) to TH2 (anti-inflammatory). Several studies have demonstrated that IL-1 β aggregates around AuNPs, thus decreasing the number of available IL-1 β molecules that interact with the interleukin cellular receptor and altering its biological activity (38, 39).

Based on these data, the present study evaluated the antioxidant and anti-inflammatory effects of *Viburnum opulus* extract-capped gold nanoparticles (AuNP-VO) in a model of experimental carrageenan-induced plantar inflammation in Wistar rats. The effects were assessed by oxidative stress and inflammation markers, and by histopathological analysis of inflamed plantar tissue.

Material and methods

Reagents

Type IV lambda-carrageenan, indomethacin, carboxymethylcellulose, o-phthalaldehyde, 2-thiobarbituric acid, Bradford reagent, t-butyl hydroperoxide, and glutathione reductase were obtained from Sigma-Aldrich Chemicals GmbH (Germany). EDTA-Na₂ was purchased from Merck KGaA Darmstadt (Germany) and absolute ethanol and EDTA-Na₂ were purchased from Chimopar (Bucharest). ELISA tests for cytokines (TNF- α , IL-1 β , IL-1 α , IL-6, and IL-10) were purchased from Luminex Corporation (Austin, TX, USA). Antibodies against COX-2, iNOS, and glyceraldehyde 3-phosphate dehydrogenase (GAPDH) were procured from Santa Cruz Biotechnology (Santa Cruz, CA, USA). All reagents were of high-grade purity.

Preparation and characterization of fruit extract

Viburnum opulus (VO) fruits were harvested in August 2019, packed in polyethylene bags, and frozen until use. The concentrated fruit extract was obtained as follows: 100 g of fruit puree was stirred for one hour at room temperature with 300 mL of acetone, the mixture was filtered, and the acetone was completely removed under vacuum. The resulting concentrated fruit extract was further used for *the in vivo* antioxidant and anti-inflammatory evaluation of VO fruits. The concentrated fruit extract was characterized using the total phenolic content, determined by the Folin–Ciocalteu method (40), slightly modified by Moldovan et al. (41). Thus, 250 μ L of diluted fruit extract (256 fold) was mixed with 1.5 mL of Folin–Ciocalteu reagent. After 5 minutes, 1.2 mL of 0.7M sodium carbonate solution was added to the mixture. The resulting solution was kept at room temperature in the dark for 2 h and then spectrophotometrically evaluated by measuring absorbance at 765 nm. A calibration curve of the gallic acid standard was used to determine the total phenolic content of the investigated fruit extract.

Preparation and characterization of gold nanoparticles

AuNPs were obtained by a green procedure that involves the reduction of Au^{3+} ions using the antioxidant phyto-compounds of VO fruits. To this end, at 25 mL diluted fruit extract 100 mL of boiling 1 mM HAuCl_4 solution were added and the resulting mixture was stirred for 1 h. The progress of the reduction reaction was visually and spectrophotometrically evaluated using a Perkin-Elmer Lambda 25 UV-Vis double-beam spectrophotometer. The color change from faint red to intense purple indicates the formation of a colloidal gold solution. The AuNPs were purified by repeated centrifugation at 10.000 rpm and washed. Several consecrated methods have been used to evaluate the properties of the synthesized gold nanoparticles, including UV-Vis spectroscopy, transmission electron microscopy (TEM), dynamic light scattering (DLS) and zeta potential. An H-7650 120 kV automatic TEM Hitachi microscope on a carbon-coated copper grid was used to investigate the size and morphology of the AuNPs, and the hydrodynamic diameter and zeta potential were determined using a Zetasizer Nano ZS-90 instrument (Malvern Instruments Ltd., Malvern, UK) equipped with a He–Ne laser.

Experimental design

28 male Wistar rats, weighing 110–130 g, from the Biobase of the University of Medicine and Pharmacy

‘Iuliu Hațieganu’ Cluj-Napoca were used in the study. For acclimatization, the animals were kept for one week before the start of the experiments in the Biobase of the Department of Physiology under the following conditions: light/dark cycle of 12 h/12 h, controlled temperature of 21 ± 2 °C, and water and food *ad libitum*. The experiments were carried out in compliance with the protocols approved by the Ethics Commission of UMF ‘Iuliu Hațieganu’ in accordance with internationally accepted principles for the use and handling of laboratory animals (European Community Guidelines, EEC Directive of 1986; 86/609/EEC).

The experimental model used was carrageenan-induced paw inflammation, as described by Winter et al. (42). Animals were randomized into 4 groups ($n = 7$) as follows: control group, treated with vehicle (phosphate buffered saline - PBS); group treated with 5 mg/kg b.w. Indomethacin; group treated with 15 mg/kg b.w. *Viburnum opulus* (VO) extract; group treated with 0.3 mg/kg b.w. gold nanoparticles (AuNP-VO). All compounds were orally administered daily for 4 days. On day 5, inflammation of the paw with sterile 1% carrageenan suspension was induced in all groups. Under intraperitoneal anesthesia with ketamine/xylazine (90 mg/kg b.w./10 mg/kg b.w. xylazine), each animal was injected into the right paw under the aponeurosis with 100 μ L carrageenan suspension. The left paw was injected with an equal volume (100 μ L) of PBS.

The doses used were selected based on previous pilot studies on Wistar rats (43). Indomethacin (no. 17378), a potent nonsteroidal anti-inflammatory agent, was suspended in 1.5% carboxymethylcellulose. The dose was chosen based on previous studies and served as the positive control (44). Saline phosphate buffer (PBS) was used as a negative control.

At 2, 24, and 48 h after carrageenan administration, blood and plantar tissues were collected under anesthesia. Part of the plantar tissues was immersed in formalin and processed for histopathological examination, and part was homogenized with a Polytron homogenizer (Brinkman Kinematica, Switzerland) for 3 min, on ice, in phosphate buffered saline (pH 7.4) in a 1:4 ratio (w/v) for biochemical evaluation. COX-2 and iNOS expression was evaluated by western blotting, and the profile of proinflammatory and anti-inflammatory cytokines in plantar tissue was quantified by ELISA. Oxidative stress markers were determined from blood and plantar tissue homogenates. Protein concentration in the homogenate was measured using the Bradford method (45).

Measurement of paw edema

Paw edema was assessed using a plethysmometer (Ugo Basile, 37140, Italy). For this, paw volume was measured

initially and then at 2, 24, and 48 h after carrageenan injection. The anti-inflammatory activity was assessed as a percentage of the reduction in edema in the treated groups, compared to the control group (46), according to the formula:

$$\begin{aligned} \text{Anti-inflammatory activity\%} \\ = [1 - (\text{treated paw volume}/\text{control paw volume})] \\ \times 100 \end{aligned}$$

Oxidative stress assessment

Malondialdehyde (MDA) (47), reduced glutathione (GSH) (48), catalase (CAT) (49), and glutathione peroxidase (GPx) activities (50) were measured in the blood and skin tissue homogenates. The reduced glutathione/oxidized glutathione ratio (GSH/GSSG) was calculated.

Histopathology exam and lesion grading

Paw biopsies were fixed in 10% neutral-buffered formalin for at least 24 h before trimming and routine processing. Serial tissue sections (5 μm thick) were stained with hematoxylin and eosin (HE). Each case had five different sections of plantar tissue examined using an Olympus system (microscope, digital camera, and image software). Histology scores were assigned on a scale from 0 (normal) to 5 (most severe), based on the presence, intensity, and type of cell infiltrate, edema, necrosis, and hemorrhage (51). The paw inflammation scores for each group were averaged and analyzed.

The assessment of COX-2 and iNOS in the paw tissue

For quantification of cyclooxygenase (COX)-2 and inducible nitric oxide synthase (iNOS), western blotting was performed. For western blotting, lysates (20 μg protein/band) were separated by electrophoresis (SDS-PAGE) and transferred by adsorption onto a polyvinylidene difluoride membrane using the Bio-Rad Miniprotean system (Bio-Rad, Hercules, CA, USA) as previously described (52). The blots were blocked at room temperature for one hour and incubated overnight with primary anti-COX-2, anti-iNOS, and anti-GAPDH antibodies. After washing, the blots were incubated with specific secondary antibodies for 1.5 h. Protein visualization was accomplished using the West Femto Chemiluminescent Supersignal substrate (Thermo Fisher Scientific, Rockford, IL, USA), and the measurement was performed using Image Lab analysis software (Bio-Rad, Hercules, CA, USA). GAPDH was used as a control for protein loading.

Cytokine profile analysis

IL-1 α , IL-1 β , IL-6, IL-10, and TNF α levels in skin tissue were determined using a multiplex cytokine kit (Luminex 200; Luminex Corporation, Austin, TX, USA). The assay was performed according to the manufacturer's instructions.

Data analysis

The obtained data were statistically processed using GraphPad Prism version 5.0 for Windows (GraphPad Software, San Diego, CA, USA), performing one-way ANOVA followed by Tukey's post-hoc test. The threshold significance level was set at $p < 0.05$ (* $p < 0.05$, ** $p < 0.01$, *** $p < 0.001$).

Results

Synthesis and characterization of gold nanoparticles

In the present study, the VO fruit extract was used as a source of reducing agents for gold ions and stabilizing agents for the synthesized nanoparticles. *Viburnum opulus* L. fruits are well known for their high antioxidant properties because of their high content of polyphenolic compounds (53, 54). The determined value of the TPC of the fruit extract was 22.54 GAE/L. This high content enabled us to select this extract for the synthesis of AuNPs. By adding the VO fruit extract to the gold ion solution, a rapid color change from faint red to intense purple was observed, indicating the reduction of metallic ions and the synthesis of gold nanoparticles. The UV-Vis absorption spectrum of AuNP-VO (Figure 1A) displays an intense peak at $\lambda_{\text{max}} = 536 \text{ nm}$, confirming the formation of a gold colloidal solution. This maximum absorption peak is due to the SPR band characteristic of the nanogold, which is consistent with other studies on green synthesis of AuNP-VO (55, 56).

The size and morphology of the synthesized AuNP-VO were evaluated by TEM. The results are shown in Figure 1. As shown in Figure 1B, the obtained AuNPs were spherical in shape, homogeneous, and not aggregated, with an average size of 65 nm (Figure 1C).

The hydrodynamic size and stability of the AuNP-VO were assessed using DLS/zeta potential analysis. The obtained value of the zeta potential (-20.7 mV , Figure 2A) clearly indicates the negative charge of the surface of the nanoparticles due to the presence of biomolecules from the fruit extract proving their good stability. The average hydrodynamic size determined by DLS was 83 nm (Figure 2B).

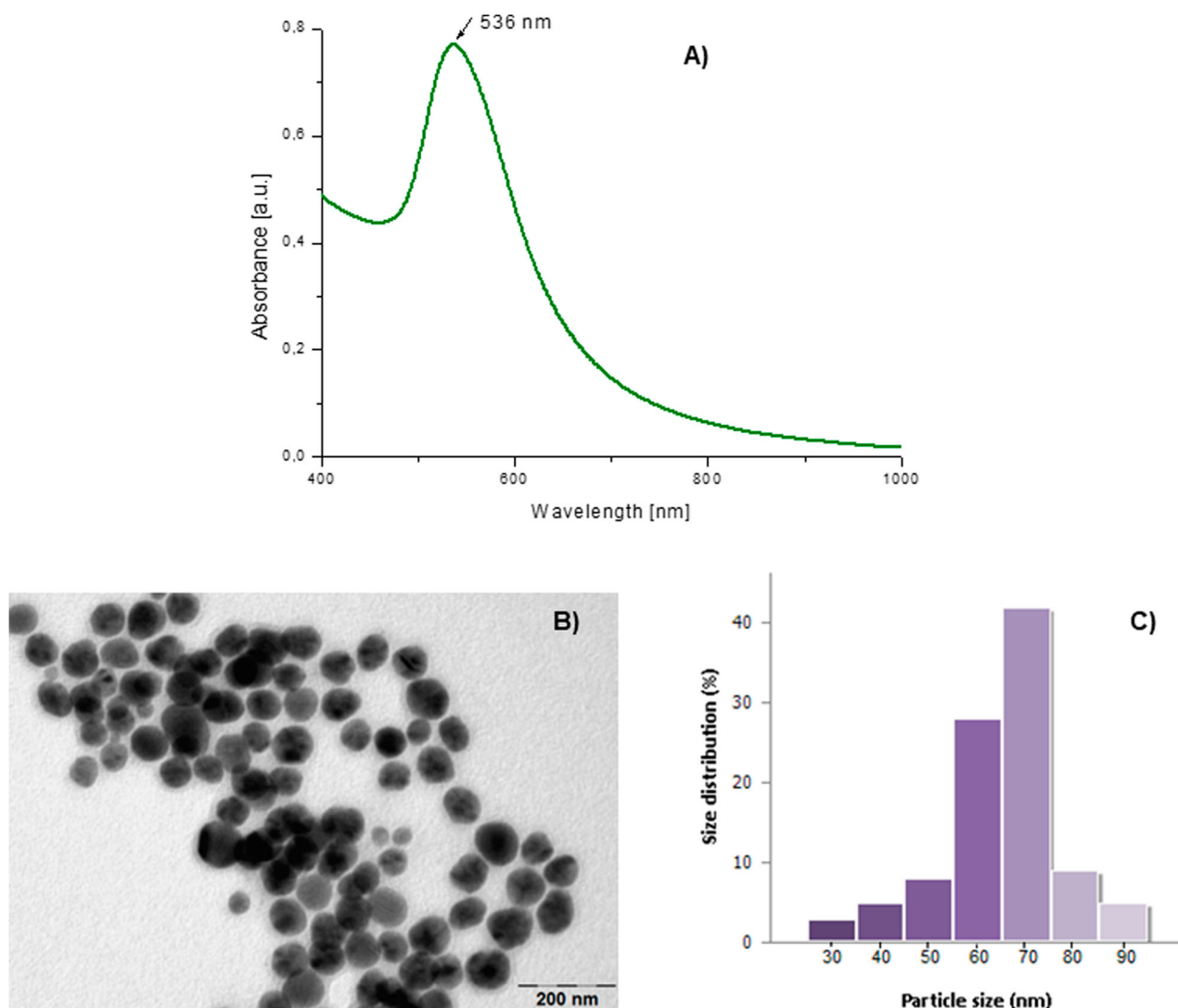


Figure 1. UV-Vis spectrum of the synthesized AuNP-VO (A). Characterization of the synthesized AuNP-VO: TEM image (B); histogram (C).

Measurement of paw edema

Plantar injection of carrageenan induced a significant increase in paw edema, which peaked after 2 h. Paw edema persisted for up to 48 h after treatment. Pre-

administration of the VO extract for 4 days significantly decreased paw edema only at 2 h ($p < 0.01$), and the values were close to those obtained after administration of indomethacin at 2 h ($p < 0.05$). After 24 and 48 h,

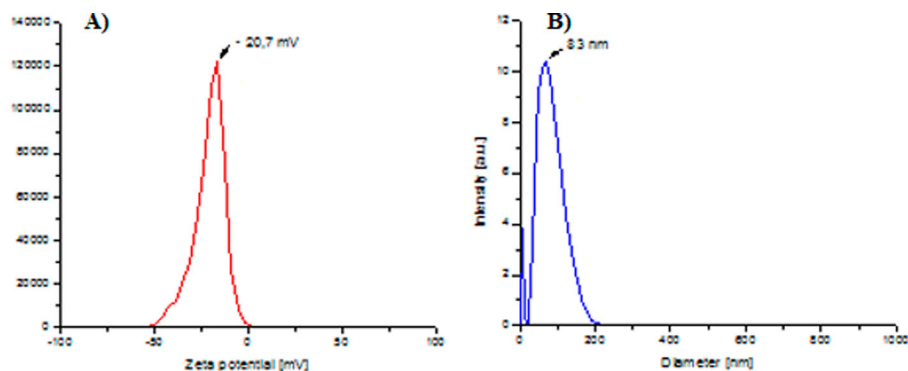


Figure 2. Characteristics of the obtained AuNP-VO: (A) zeta potential and (B) hydrodynamic diameter.

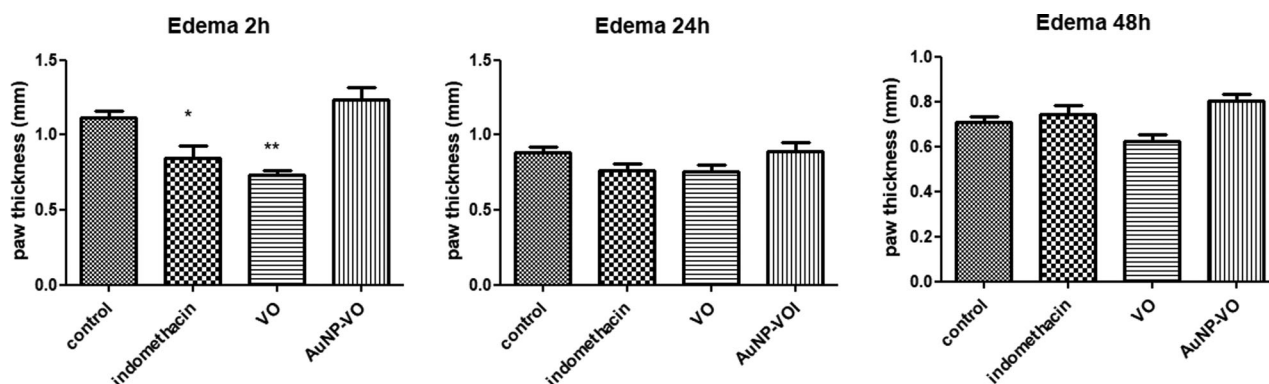


Figure 3. Paw volume at 2 h, 24 h and 48 h after carrageenan administration. At 2 h, paw edema was lower in the Indomethacin ($p < 0.05$) and VO ($p < 0.01$) groups compared to the control group. The statistical significance between the compared groups was evaluated with one-way ANOVA followed by the Tukey-test, * $p < 0.05$, ** $p < 0.01$ vs control group.

none of the treatments administered did not changed the clinical plantar edema ($p > 0.05$) (Figure 3).

Biochemical assays

In the serum, MDA decreased significantly in all treated groups compared to the control group, both at 2, 24, and 48 h after carrageenan administration ($p < 0.001$) (Figure 4A).

In the plantar tissue, MDA levels increased significantly at 2 h in the groups treated with indomethacin and AuNP-VO ($p < 0.001$), while the VO extract reduced lipid peroxidation close to the control level. MDA values decreased after AuNP-VO treatment only at 48 h, similar to indomethacin ($p < 0.001$) (Figure 4B). The VO extract maintained low levels of MDA up to 24 h after carrageenan injection, while at 48 h, its protective effect was minimal.

In serum, the GSH/GSSG ratio was enhanced 2 h after carrageenan administration in all treated groups compared to the control group, with an increase maintained in the VO and AuNP-VO groups up to 24 h ($p < 0.001$) and 48 h ($p < 0.01$) (Figure 5A).

In paw tissue, at 2 and 24 h, the GSH/GSSG ratio was improved after AuNP-VO treatment compared to the control group ($p < 0.001$), while at 48 h, the values were close to those of the control group. At 24 h, after the administration of carrageenan, the GSH/GSSG ratio increased in the indomethacin-treated group, and this increase was maintained at 48 h ($p < 0.001$) (Figure 5B), suggesting a beneficial effect on endogenous antioxidant defense.

CAT activity was enhanced at 2 h in VO-treated animals compared with that in animals receiving indomethacin or AuNP-VO ($p < 0.01$). Enzymatic activity was amplified at 24 h in the paw tissue of AuNP-VO-treated animals ($p < 0.05$) and maintained for up to 48 h ($p < 0.001$) (Figure 6A).

GPx activity decreased at 2 and 24 h in the indomethacin-treated group ($p < 0.01$) and in the VO group ($p < 0.05$) compared to that in the control. At 48 h, AuNP-VO administration significantly increased enzymatic activity compared to that in the control group ($p < 0.001$) and the other groups ($p < 0.01$) (Figure 6B).

Cytokine profile analysis

At 2 h after the induction of inflammation, IL-1 α levels decreased after treatment with VO ($p < 0.01$) and AuNP-VO ($p < 0.001$) compared to controls, while indomethacin administration significantly increased IL-1 α secretion ($p < 0.01$). At 48 h, AuNP-VO induced a significant increase in IL-1 α levels compared with all other groups ($p < 0.001$) (Figure 7A).

IL-1 β decreased in all treated groups compared to the control group 2 h after induction of inflammation; the decrease was more significant in the group that received VO ($p < 0.001$). At 48 h, this decrease was maintained in the VO group compared to that in all other groups ($p < 0.001$) (Figure 7B). IL-6 levels diminished in all groups only at 2 h (indomethacin $p < 0.05$; VO $p < 0.001$; AuNP $p < 0.01$, vs. control), whereas at 24 h and 48 h, there were no significant differences between these groups (Figure 7C).

IL-10, an anti-inflammatory cytokine, and TNF α secretion decreased in the VO and AuNP-VO groups ($p < 0.01$) only 2 h after inflammation. At 24 and 48 h, there were no significant differences between the groups (Figure 8A, 8B).

The assessment of COX-2 and iNOS in the paw tissue

iNOS expression decreased at 2 h in the indomethacin-treated group ($p < 0.001$) and the AuNP-VO group ($p <$

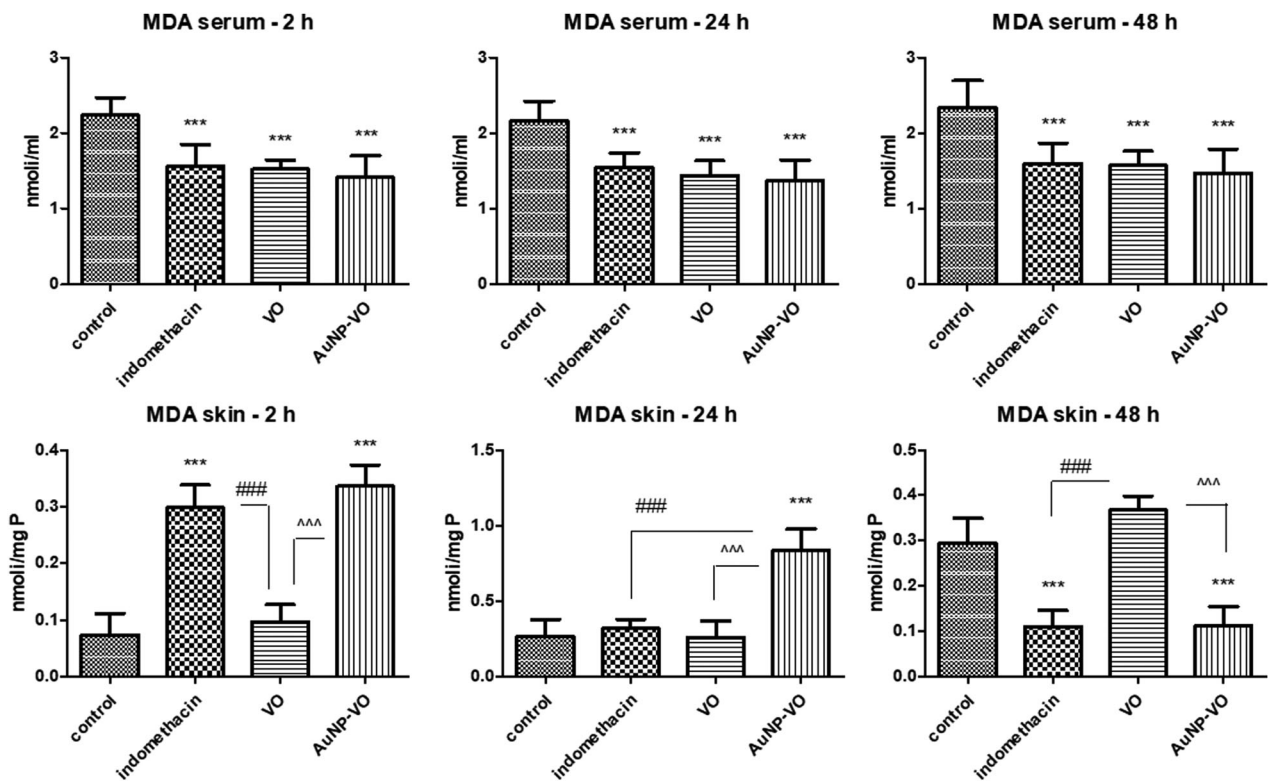


Figure 4. Malondialdehyde in serum (A) and plantar tissue (B) at 2 h, 24 h and 48 h after carrageenan administration. A. In serum, MDA diminished in all treated groups at all intervals, compared to the control group ($p < 0.001$). B. In the plantar homogenates, MDA level increased at 2 h and then decreased at 48 h in the Indomethacin and AuNP-VO groups, compared to the control group and VO group ($p < 0.001$). The statistical significance between the compared groups was evaluated with one-way ANOVA followed by the Tukey-test, $***p < 0.001$ vs control group; $###p < 0.001$ vs Indomethacin group; $^^^p < 0.001$ between VO and AuNP-VO.

0.05) compared with the control group. At 24 h, iNOS expression increased in the VO and AuNP-VO-treated groups compared to the control group or the indomethacin group ($p < 0.001$) (Figure 9).

COX-2 expression decreased significantly at 2 h in all treated groups ($p < 0.001$) compared with that in the control group. At 24 h, COX-2 levels remained low in the indomethacin and AuNP-VO groups ($p < 0.001$), while at 48 h, COX-2 levels increased in the indomethacin-treated group ($p < 0.001$) and AuNP-VO-treated group ($p < 0.05$) compared to those in the control group or the VO-treated group (Figure 10).

Histopathology analysis

Minimal histological changes in paw biopsies were observed in all animals from the treated groups, but not in the untreated control. They varied among individuals and were composed of a combination of the following: focal to multifocal to diffuse inflammatory infiltrates (mainly macrophages, lymphocytes, and plasma cells) affecting all layers, increased numbers of mast cells, edema, necrosis, and focal hemorrhage (Figure 11). At 2 and 24 h, subcutaneous edema was more severe in

the control, VO, and AuNP-VO groups, while it was less prominent in the indomethacin group. Overall edema was reduced at 48 h in all groups. Inflammatory infiltrates, mainly lymphocytes and plasma cells, with rare neutrophils and macrophages, were observed in all groups at all experimental times. They were minimal in the indomethacin-treated group across all experimental times ($p < 0.01$, 2 h; $p < 0.001$ at 24 h and $p < 0.001$ at 48 h vs. control group) and most severe in the control group, whereas VO and AuNP-VP were of intermediate intensity. Thus, in the VO and AuNP-VO groups, the average inflammatory score was lower than that in the control group at 24 h ($p < 0.05$, $p < 0.01$) and was maintained at 48 h after induction of inflammation ($p < 0.001$ and $p < 0.01$).

The histopathological quantification of the paw changes is illustrated in Table 1.

Discussion

Carrageenan-induced paw edema is an experimental model of acute inflammation used to quantify the potential anti-inflammatory effects of drugs or natural compounds. In the present study, we evaluated the

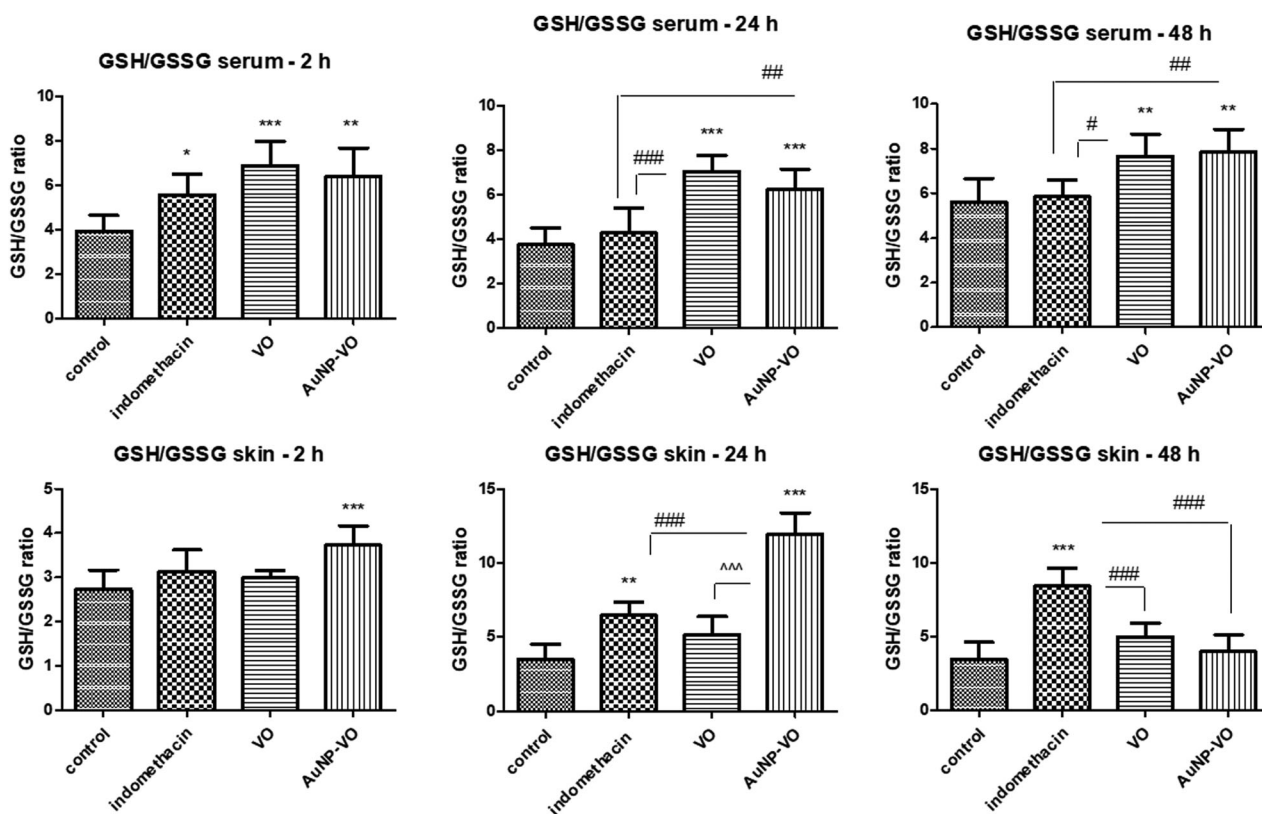


Figure 5. GSH/GSSG ratio in serum (A) and plantar tissue (B) at 2 h, 24 h and 48 h after carrageenan administration. A. In serum, the GSH/GSSG ratio increased at 2 h in all treated groups compared to the control group; the VO and AuNP-VO groups showed increases in the GSH/GSSG ratio at 24 h ($p < 0.001$) and at 48 h ($p < 0.01$). B. In the paw tissue, the GSH/GSSG ratio enhanced at 2 h in the AuNP-VO group compared to the control group ($p < 0.001$) and at 24 h compared to all groups ($p < 0.001$). At 48 h, the GSH/GSSG ratio decreased in AuNP-VO-treated group while in the Indomethacin group, the values were maintained increased compared to the other groups ($p < 0.001$). The statistical significance between the compared groups was evaluated with one-way ANOVA followed by the Tukey-test, * $p < 0.05$, ** $p < 0.01$, *** $p < 0.001$ vs control group; # $p < 0.05$, ## $p < 0.01$, ### $p < 0.001$ vs Indomethacin group; ^^ $p < 0.001$ between VO and AuNP-VO.

anti-inflammatory and antioxidant effects of gold nanoparticles phytoreduced with *Viburnum opulus* fruit extract compared to indomethacin and *Viburnum opulus* fruit extract.

A green synthesis method of gold nanoparticles was applied, by exploiting the reducing potential of the bioactive compounds from the above-mentioned fruits. Numerous plant extracts have been used for the green phyto-mediated synthesis of AuNPs. The involvement of biomolecules from plants throughout the synthesis process is an efficient and eco-friendly method for obtaining metal nanoparticles (44, 57). Apart plants (58, 59, 27, 33), different biological sources such as algae, fungi, yeasts, bacteria or viruses can be used for the intra- or extracellular biosynthesis of metallic nanoparticles (24, 25, 60, 61, 62, 63). This eco-friendly method for fabrication of metallic nanoparticles presents numerous benefits over traditional chemical and physical methods, offering a clean, benign, nontoxic, cost-effective and relatively easy to scale up method of obtaining well-

defined nanoparticles with a wide range of shapes, sizes, compositions and properties (26, 61).

The results showed that the effect of AuNP-VO on plantar oxidative stress appeared 48 h after the induction of inflammation. Thus, AuNP-VO reduced skin MDA formation and increased CAT and GPx activities as well as the GSH/GSSG ratio, particularly in late-stage inflammation. Additionally, AuNP-VO diminished the local secretion of IL-1 α , IL-1 β , IL-6, and TNF- α compared to the control group at 2 h after induction of inflammation with moderate reduction in iNOS and COX-2 expression. The effect was persistent for COX-2 for up to 24 h. VO treatment diminished MDA levels in the paw, especially at 2 and 24 h after carrageenan injection, in parallel with the increase in CAT activity and reduced IL-1 α , IL-1 β , IL-6, and TNF- α levels, mainly at 2 h. In addition, the VO extract diminished the expression of iNOS and COX-2 in plantar tissue at 2 and 48 h after carrageenan injection and reduced IL-10 secretion. Moreover, protection against oxidative stress was important in serum for

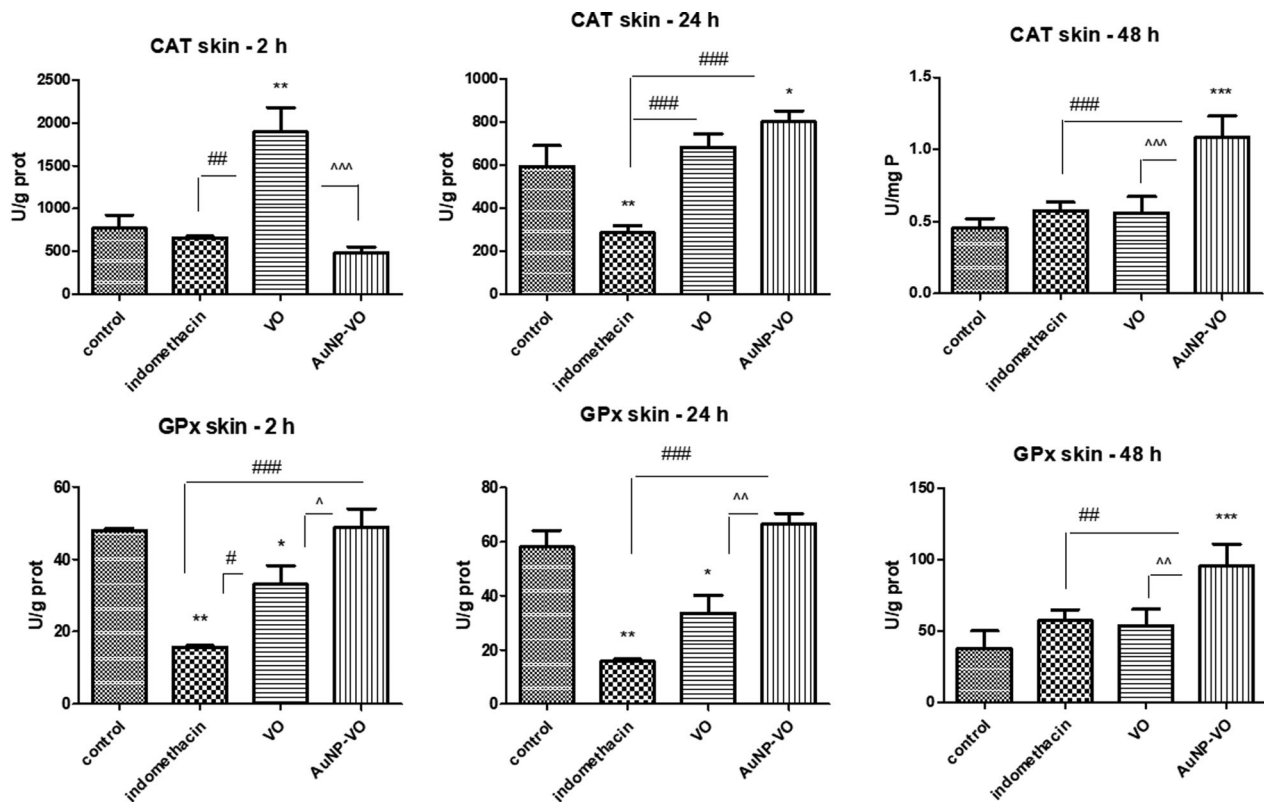


Figure 6. Catalase (A) and glutathione peroxidase (B) activities in plantar tissue at 2 h, 24 h and 48 h after carrageenan administration. CAT activity increased at 2 h in the VO-treated group ($p < 0.01$) and at 48 h in the group receiving AuNP-VO ($p < 0.001$), compared to controls. GPx activity was improved 48 h after AuNP-VO treatment ($p < 0.001$ vs. control group; $p < 0.01$ vs. Indomethacin group). The statistical significance between the compared groups was evaluated with one-way ANOVA followed by the Tukey-test, * $p < 0.05$, ** $p < 0.01$, *** $p < 0.001$ vs control group; ## $p < 0.01$, ### $p < 0.001$ vs Indomethacin group; ^^ $p < 0.001$ between VO and AuNP-VO.

both VO and AuNP-VO, suggesting a beneficial effect on systemic changes induced by local inflammation.

Histologically, paw edema was reduced in the indomethacin, VO, and AuNP-VO groups at all experimental times, with a progressive reduction in intensity from 2 h to 24 h to 48 h in each group. Inflammatory infiltrates showed an opposite trend to edema in all groups, with mixed inflammatory cells increasing progressively with time. However, when edema and inflammation, together with other histological changes, were combined to obtain the inflammatory score, there was a steady increase in the score from 2 h to 24 h to 48 h in all groups except VO. All treated groups showed a reduction in the inflammatory score, and indomethacin showed the best protective effect histologically. At 48 h, VO and indomethacin had similar and low scores, and exerted the same morphological protection.

Carrageenan administration induces a biphasic inflammatory response; in the early phase, histamine, serotonin, and bradykinin are released, while the late phase includes the production of free radicals from neutrophils and macrophages, the secretion of cytokines, NO synthesis, neutrophil infiltration, COX-2 activation, and the subsequent production of prostaglandins (11).

Previous studies have shown that carrageenan administration in mice triggers intense inflammatory events characterized by excessive excretion of various inflammatory mediators, temporary vasoconstriction, and vasodilation with edema, which peaks after 8 h (64, 65). In our study, edema was maximum at 2 h after carrageenan administration and then decreased at 24 h and 48 h. VO extract significantly reduced clinical edema at 24 h, while at 48 h, the effect was not significant.

Redox imbalance was quantified by MDA level and GSH/GSSG ratio in serum and plantar tissue and by evaluation of antioxidant enzyme activities. MDA is a specific marker of lipid peroxidation and its production is a valuable marker for monitoring oxidative stress. The GSH system represents the first line of endogenous antioxidant defense against free radicals and is mostly found in the reduced form (GSH) and only a small part in the oxidized form (GSSG). The GSH/GSSG ratio reflects the redox equilibrium. Catalase (CAT) and glutathione peroxidase (GPx) are among the primary antioxidant enzymes that detoxify excessive hydrogen peroxide and lipid peroxides in cells.

The results of our study showed an improvement in systemic antioxidant defense in the groups treated

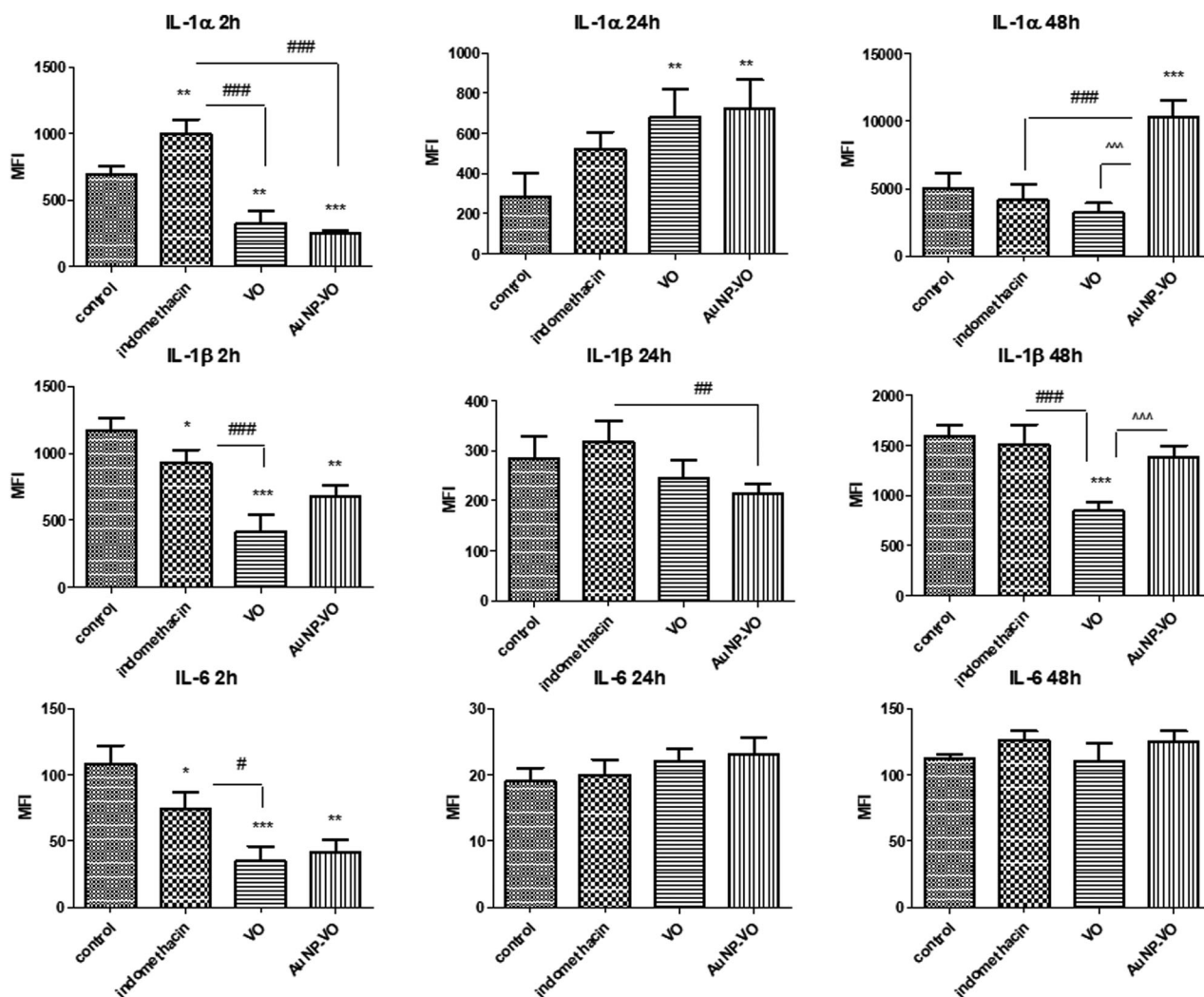


Figure 7. IL-1 α (A), IL-1 β (B), and IL-6 (C) levels in plantar tissue at 2, 24, and 48 h after carrageenan administration. The levels of IL-1 α , IL-1 β , and IL-6 were significantly reduced at 2 h in the groups treated with VO extract ($p < 0.01$) and AuNP-VO ($p < 0.001$) compared to the control group. Low IL-1 β levels were maintained at 24 h ($p < 0.01$) in the AuNP-VO-treated group compared with indomethacin, while at 48 h, cytokine secretion decreased in the VO-treated group ($p < 0.001$) compared to the other groups. IL-1 α levels increased at 24 h in the VO- and AuNP-VO-treated groups ($p < 0.001$), and increased at 48 h in the AuNP-VO-treated group ($p < 0.001$). The statistical significance between the compared groups was evaluated with one-way ANOVA followed by Tukey's test, ** $p < 0.01$, *** $p < 0.001$ vs. control group; ### $p < 0.001$ vs. indomethacin group; ^^ $p < 0.001$ between VO and AuNP-VO.

with VO and AuNP-VO compared to the control group. In the plantar tissue, the effect was dependent on the compound administered and the time of evaluation. VO extract reduced lipid peroxidation and enhanced antioxidant defense early after induction of inflammation, whereas AuNP-VO exerted a late effect 48 h after the induction of inflammation.

The literature on the protective effect of VO extract in pathological conditions is contradictory. Thus, some studies showed favorable effects of VO fruit extract while the others exhibited the lack of its effect. In an *in vivo* rat experiment, Eken et al. (66) demonstrated protective properties against ischemia/reperfusion-induced oxidative stress during lung transplantation.

Intraperitoneal administration of 200 mg/kg b.w. VO dried fruit extract resulted in significant increases in superoxide dismutase (SOD), CAT, GPx, and GSH levels, and decreased MDA and carbonylated protein levels.

In vitro studies have also shown favorable effects of VO fruit extract, with decreased intracellular reactive oxygen species production in human Caco-2 adenocarcinoma cells (19), MIN6 mouse cells, and 3T3-L1 cells (21, 22).

In contrast, Altun et al. (67), in rats and mice with plantar inflammation induced by carrageenan, VO leaf extract did not have a protective effect on inflammation compared to Indomethacin, independent of dose used (50 mg, 100 mg or 200 mg/kg b.w.). The divergent

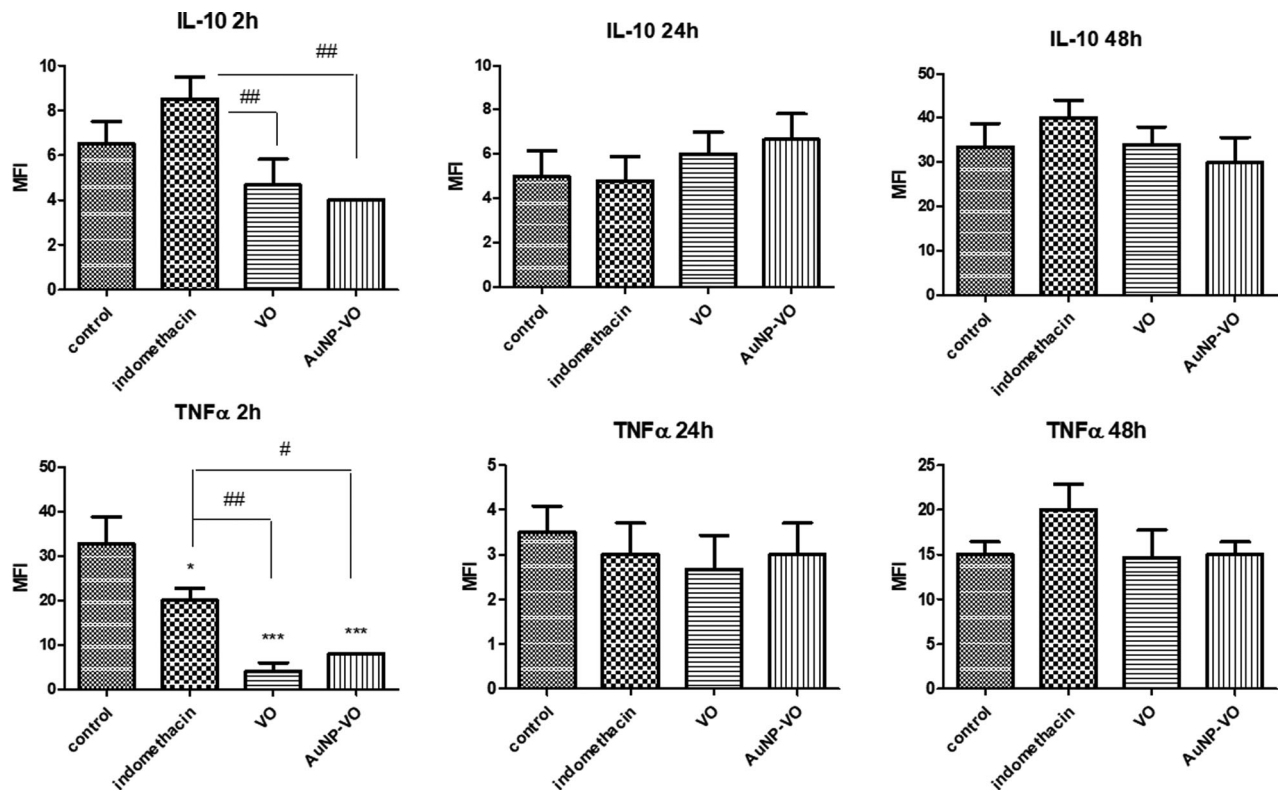


Figure 8. IL-10 (A) and TNF α (B) levels in the plantar tissue at 2 h, 24 h and 48 h after carrageenan administration. IL-10 ($p < 0.01$) and TNF α ($p < 0.01$ and $p < 0.05$) levels decreased at 2 h after carrageenan administration in animals treated with VO and AuNP-VO compared to Indomethacin group. The statistical significance between the compared groups was evaluated with one-way ANOVA followed by the Tukey-test, * $p < 0.05$, *** $p < 0.001$ vs control group; # $p < 0.05$, ## $p < 0.01$ vs Indomethacin group.

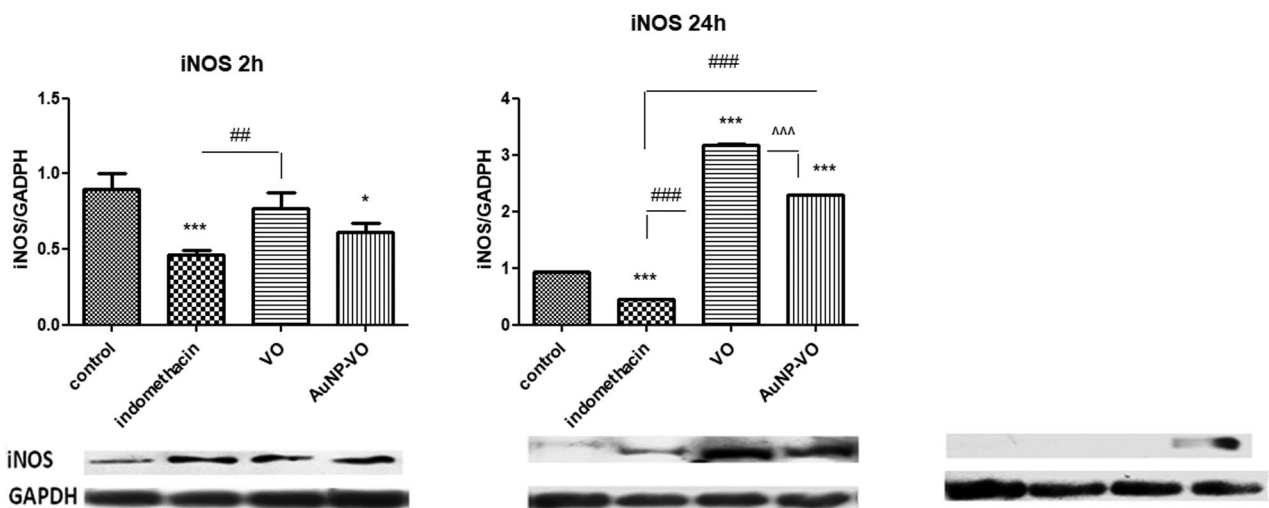


Figure 9. iNOS expressions in animal paw tissues at 2 h, 24 h and 48 h after carrageenan administration. Image analysis of WB bands was performed through densitometry (lower panel). Results normalized to GAPDH were shown in upper panel. At 2 h, iNOS expression decreased in the Indomethacin ($p < 0.001$) and AuNP-VO ($p < 0.05$) groups compared to the control group. At 24 h, iNOS increased in VO and AuNP-VO groups compared to control group or Indomethacin group ($p < 0.001$). At 48 h, Indomethacin, VO and AuNP-VO did not induce the iNOS expression. The statistical significance between the compared groups was evaluated with one-way ANOVA followed by the Tukey-test, * $p < 0.05$, *** $p < 0.001$ vs control group; # $p < 0.01$, ### $p < 0.001$ vs Indomethacin group; ^^^ $p < 0.001$ between VO and AuNP-VO.

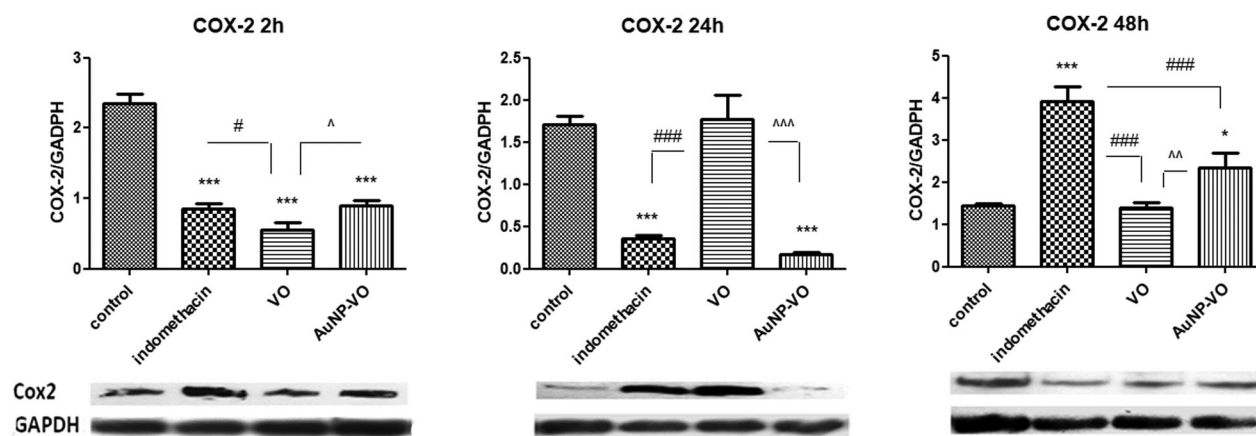


Figure 10. COX-2 expressions in the paw tissues at 2 h, 24 h and 48 h after carrageenan administration. Image analysis of WB bands was performed through densitometry (lower panel). Results normalized to GAPDH were shown in upper panel. At 2 h, COX-2 expression decreased in all treated groups compared to the control group. At 24 h the COX-2 values diminished in the Indomethacin and AuNP-VO groups compared to the control or VO group ($p < 0.001$). At 48 h, COX-2 increased in the Indomethacin group ($p < 0.001$) and in the AuNP-VO group ($p < 0.05$) compared to the control group or the VO group. The statistical significance between the compared groups was evaluated with one-way ANOVA followed by the Tukey-test, $*p < 0.05$, $***p < 0.001$ vs control group; $\#p < 0.05$, $###p < 0.001$ vs Indomethacin group; $\wedge p < 0.05$, $\wedge\wedge p < 0.01$, $\wedge\wedge\wedge p < 0.001$ between VO and AuNP-VO.

literature data can be explained by the different contents of polyphenols in the VO extract used and the time of quantification of the effects, especially as its effect is short-lived.

IL-1 α , IL-1 β , IL-6, and TNF- α are the main pro-inflammatory cytokines responsible for the early inflammatory responses. Early stage mediators are generally produced by platelets and mast cells and play a role in inducing

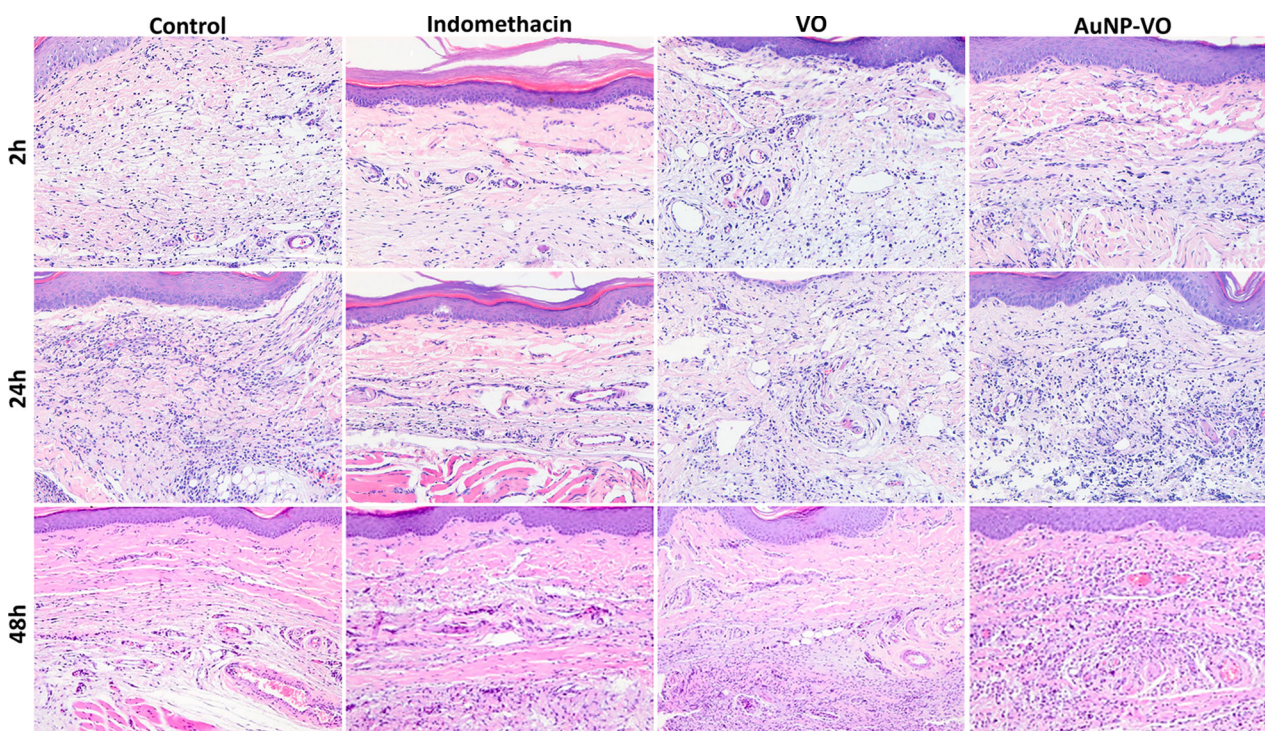


Figure 11. Paw changes histologically at 2 h, 24 h and 48 h after carrageenan administration. Prominent subcutaneous edema and mixed inflammatory infiltrates in the dermis and subcutis in the control, VO and AuNP-VO groups at 2 and 24 h, and minimal in the Indomethacin treated group. Edema and inflammation were reduced at 48 h across all groups but were significant compared to control group. HE stain x ob 40.

Table 1. Grading of paw lesions (inflammatory score average per group).

	Control	Indomethacin	VO	AuNP-VO
2 h	1.39 ± 0.20	0.5 ± 0.15**	1.44 ± 0.26	1.33 ± 0.21
24 h	2.11 ± 0.11	0.61 ± 0.12***	1.56 ± 0.18*	1.44 ± 0.19**
48 h	2.02 ± 0.05	0.64 ± 0.18***	0.67 ± 0.22***	1.59 ± 0.24**

Where * $p < 0.05$; ** $p < 0.01$; *** $p < 0.001$.

and activating the inflammatory process. Late-stage mediators are involved in controlling vascular phenomena. They appear later, 6–12 h after the onset of inflammation and are represented by various arachidonic acid derivatives (16, 17, 68).

The results of our study confirmed important anti-inflammatory effects compared to indomethacin, both for VO extract and AuNP-VO 2 h after induction of inflammation. This effect was not persistent at 24 or 48 h, less in terms of COX-2, which was reduced after carrageenan administration.

Jeon et al. (69) showed that AuNPs exert immunomodulatory effects through their ability to block NF- κ B activation by suppressing the production of pro-inflammatory cytokines IL-1 β and TNF- α . In another study, Ma et al. (70) showed that AuNPs decreased iNOS-induced gene expression and NO production by blocking NF- κ B and STAT1 activation in lipopolysaccharide-stimulated RAW264.7 cells. Sumbayev et al. (38) demonstrated the size-dependent anti-inflammatory activity of AuNPs by downregulating IL-1 β -induced cellular responses in both *in vitro* and *in vivo* studies. AuNPs with a diameter of 5 nm completely inhibited the inflammatory process, those with a diameter of 15 nm showed moderate efficacy, and those with a diameter of 35 nm did not show any statistically significant effect. The large size of our AuNPs could explain the moderate anti-inflammatory effect obtained in the experiment.

Several *in vitro* studies have shown antioxidant and anti-inflammatory effects of 3–5 nm AuNP (HUVECs, VECs) (71), or for 15 nm, 20 nm, and 50 nm AuNPs (RAW264.7 cells) (39, 70, 72). Khan and Khan (73) also observed the antioxidant and anti-inflammatory effects of AuNPs with sizes of 20 nm in rats with collagen-induced arthritis. They exhibited a decrease in MDA levels and a significant decrease in the mRNA expression of NF- κ B, TNF- α , COX-2, iNOS, and IL-1 β . Dohnert et al. (74) showed that 10 nm AuNP have anti-inflammatory effects by significantly decreasing IL-1 β and TNF- α in an experimental model of tendinopathy in rats. Our results confirmed the moderate anti-inflammatory action of AuNP-VO with a diameter of 65 nm, especially in the early stages of inflammation, suggesting a protective effect on the secretion of histamine, bradykinin, and

serotonin from inflammatory cells. AuNP-VO inhibited cyclooxygenase-2 activity and decreased its expression both at 2 and 48 h after induction of inflammation, suggesting protection of arachidonic acid derivative generation in the late stages of paw inflammation. These results were also confirmed by histopathology, which revealed a lower inflammation score at 24 and 48 h after induction of inflammation in animals treated with AuNP-VO.

IL-10 is a cytokine with anti-inflammatory properties that limits excessive immune responses. It suppresses the release of immune mediators, antigen expression and phagocytosis (75). *In vitro* inflammation models showed that IL-10 prevents the activation of PMNs and TNF- α , as well as the release of IL-8 (76). In our study, IL-10 decreased in the groups treated with VO and AuNP-VO 2 h after induction of inflammation and was not influenced by treatment at other monitoring intervals. These data showed no effect on the secretion of anti-inflammatory cytokines.

Although several studies have reported antioxidant and anti-inflammatory effects of biologically synthesized metal nanoparticles, there are also studies that have shown genotoxic effects, which are mainly dependent on the type of metal, synthesis parameters, dose, time of administration or biological source used (61, 77). Therefore, supplementary investigations are required to decipher all mechanisms and signaling pathways involved, especially in long-term exposure, the appropriate dose used and time of administration in order to minimize side effects and increase administration safety and real benefit.

Conclusion

The results of our study demonstrate the antioxidant and anti-inflammatory effects of AuNP-VO and VO extracts on plantar inflammation, with different dynamics of action. AuNP-VO exerted antioxidant effects, especially at 48 h, and diminished the plantar inflammation in the early stages (IL-1 α , IL-1 β , IL-6, TNF- α and IL-10) but also in the late stages of inflammation (IL-1 β). The protective effects were more persistent in the plantar tissue after AuNP-VO treatment, mainly in terms of oxidative stress and arachidonic acid generation and increased local antioxidant defense. The biochemical changes were correlated with the results of the histopathological examination, where the inflammatory changes in the plantar tissue were more discrete at 24 h and 48 h after carrageenan injection. The VO extract reduced the biochemical inflammatory response, predominantly in the early stages (IL-1 α , IL-1 β , IL-6, TNF- α and IL-10), and maintained reduced IL-1 β secretion and a

lower histopathological inflammatory score at 48 h, similar to indomethacin.

Because of these properties, gold nanoparticles capped with *Viburnum opulus* and *Viburnum opulus* fruit extract can be valuable agents for the treatment of diseases associated with inflammation. Further investigations are required to accurately decipher all aspects and mechanisms involved, especially in long-term exposure to reduce side effects and increase therapeutic benefit.

Acknowledgements

We thank Mr. Remus Moldovan for handling the animals and Mrs. Nicoleta Decea for determining the oxidative stress parameters.

Disclosure statement

No potential conflict of interest was reported by the author(s).

Funding

This paper was funded by the University of Medicine and Pharmacy 'Iuliu Hatieganu' Cluj-Napoca (internal grant number 35141/17.12.2021).

Author contributions

Cristina Bidian: Conceptualization, writing the original draft. **Gabriela Adriana Filip:** conceptualization, interpretation of data, validation, supervision. **David** prepared and characterized the extract and nanoparticles. **Bianca Moldovan:** Methodology and extract characterization. **Ioana Baldea:** interpretation of data, western blotting, and validation. **Diana Olteanu** performed western blotting. **Mara Filip:** performed the experiments. **Pompei Bolfa:** histopathological analysis. **Monica Potara:** characterization of nanoparticles; **Alina Mihaela Toader:** statistical analysis. **Simona Clitici:** supervision and validation.

References

- [1] Brevetti, G.; Giugliano, G.; Brevetti, L.; Hiatt, W.R. Inflammation in Peripheral Artery Disease. *Circulation* **2010**, *122* (18), 1862–1875.
- [2] Hummasti, S.; Hotamisligil, G.S. Endoplasmic Reticulum Stress and Inflammation in Obesity and Diabetes. *Circ. Res.* **2010**, *107* (5), 579–591.
- [3] Lambrecht, B.N.; Hammad, H. The Role of Dendritic and Epithelial Cells as Master Regulators of Allergic Airway Inflammation. *Lancet* **2010**, *376* (9743), 835–843.
- [4] Vaickus, L.J.; Bouchard, J.; Kim, J.; Natarajan, S.; Remick, D.G. Oral Tolerance Inhibits Pulmonary Eosinophilia in a Cockroach Allergen Induced Model of Asthma: A Randomized Laboratory Study. *Respir. Res.* **2010**, *11* (1), 160.
- [5] Bouffi, C.; Bony, C.; Courties, G.; Jorgensen, C.; Noel, D. IL-6-dependent PGE2 Secretion by Mesenchymal Stem Cells Inhibits Local Inflammation in Experimental Arthritis. *PLoS One* **2010**, *5* (12), e14247.
- [6] Christaki, E.; Opal, S.M.; Keith, Jr., J.C.; Kessinian, N.; Palardy, J.E.; Parejo, N.A.; Lavallie, E.; Racie, L.; Mounts, W.; Malamas, M.S., et al. Estrogen Receptor Beta Agonism Increases Survival in Experimentally Induced Sepsis and Ameliorates the Genomic Sepsis Signature: A Pharmacogenomic Study. *J. Infect. Dis.* **2010**, *201* (8), 1250–1257.
- [7] Mantovani, A.; Allavena, P.; Sica, A.; Balkwill, F. Cancer-Related Inflammation. *Nature* **2008**, *454* (7203), 436–444.
- [8] Sadik, C.D.; Kim, N.D.; Luster, A.D. Neutrophils Cascading Their Way to Inflammation. *Trends Immunol.* **2011**, *32* (10), 452–460.
- [9] Sela, S.; Shurtz-Swirski, R.; Cohen-Mazor, M.; Mazor, R.; Chezar, J.; Shapiro, G.; Hassan, K.; Shkolnik, G.; Geron, R.; Kristal, B. Primed Peripheral Polymorphonuclear Leukocyte: A Culprit Underlying Chronic Low-Grade Inflammation and Systemic Oxidative Stress in Chronic Kidney Disease. *J. Am. Soc. Nephrol.* **2005**, *16* (8), 2431–2438.
- [10] Copray, J.C.; Mantingh, I.; Brouwer, N.; Biber, K.; Küst, B.M.; Liem, R.S.; Huitinga, I.; Tilders, F.J.; Van Dam, A.M.; Boddeke, H.W. Expression of Interleukin-1 Beta in Rat Dorsal Root Ganglia. *J. Neuroimmunol.* **2001**, *118* (2), 203–211.
- [11] Halici, Z.; Dengiz, G.O.; Odabasoglu, F.; Suleyman, H.; Cadirci, E.; Halici, M. Amiodarone Has Anti-Inflammatory and Anti-Oxidative Properties: An Experimental Study in Rats with Carrageenan-Induced Paw Edema. *Eur. J. Pharmacol.* **2007**, *566* (1–3), 215–221.
- [12] Moncada, S.; Higgs, A. The L-Arginine-Nitric Oxide Pathway. *N. Engl. J. Med.* **1993**, *329* (27), 2002–2012.
- [13] Nathan, C.; Xie, Q.W. Regulation of Biosynthesis of Nitric Oxide. *J. Biol. Chem.* **1994**, *269* (19), 13725–13728.
- [14] Davis, K.L.; Martin, E.; Turko, I.V.; Murad, F. Novel Effects of Nitric Oxide. *Annu. Rev. Pharmacol. Toxicol.* **2001**, *41*, 203–236.
- [15] Li, Y.Y.; Huang, S.S.; Lee, M.M.; Deng, J.S.; Huang, G.J. Anti-inflammatory Activities of Cardamonin from *Alpinia katsumadai* Through Heme Oxygenase-1 Induction and Inhibition of NF- κ B and MAPK Signaling Pathway in the Carrageenan-Induced Paw Edema. *Int. Immunopharmacol.* **2015**, *25* (2), 332–339.
- [16] Libby, P. Inflammatory Mechanisms: The Molecular Basis of Inflammation and Disease. *Nutr. Rev.* **2007**, *65* (12 Pt 2), S140–S146.
- [17] Delves, P.J.; Martin, S.J.; Burton, D.R.; Roitt, I.M. *Roitt's Essential Immunology*. 13th ed.; Wiley-Blackwell: Chichester, West Sussex, 2017.
- [18] Konarska, A.; Domaciuk, M. Differences in the Fruit Structure and the Location and Content of Bioactive Substances in *Viburnum Opulus* and *Viburnum Lantana* Fruits. *Protoplasma* **2018**, *255* (1), 25–41.
- [19] Zakłós-Szyda, M.; Pawlik, N.; Polka, D.; Nowak, A.; Koziołkiewicz, M.; Podśędek, A. *Viburnum opulus* Fruit Phenolic Compounds as Cytoprotective Agents Able to Decrease Free Fatty Acids and Glucose Uptake by Caco-2 Cells. *Antioxidants* **2019**, *8* (8), 262.

- [20] Paşayeva, L.; Arslan, A.K.K.; Kararenk, A.C. *Viburnum Opulus* L. Fruit Extracts Protect Human Neuroblastoma SH-SY5Y Cells Against Hydrogen Peroxide-Induced Cytotoxicity. *Proc. AMIA. Annu. Fall. Symp.* **2019**, *40*, 5.
- [21] Zakłos-Szyda, M.; Kowalska-Baron, A.; Pietrzyk, N.; Drzazga, A.; Podsedek, A. Evaluation of *Viburnum opulus* L. Fruit Phenolics Cytoprotective Potential on Insulinoma MIN6 Cells Relevant for Diabetes Mellitus and Obesity. *Antioxidants* **2020**, *9* (5), 433.
- [22] Podsedek, A.; Zakłos-Szyda, M.; Polka, D.; Sosnowska, D. Effects of *Viburnum opulus* Fruit Extracts on Adipogenesis of 3T3-L1 Cells and Lipase Activity. *J. Funct. Foods* **2020**, *73*, 104111.
- [23] Arasu, M.V.; Arokiyaraj, S.; Viayaraghavan, P.; Kumar, T.S.J.; Duraipandiyan, V.; Al-Dhabi, N.A.; Kaviyarasu, K. One Step Green Synthesis of Larvicidal, and azo dye Degrading Antibacterial Nanoparticles by Response Surface Methodology. *J. Photochem. Photobiol., B* **2019**, *190*, 154–162.
- [24] Salem, S.S.; Fouda, A. Green Synthesis of Metallic Nanoparticles and Their Prospective Biotechnological Applications: An Overview. *Biol. Trace Element Res* **2021**, *199*, 344–370.
- [25] Shah, M.; Fawcett, D.; Sharma, S.; Tripathy, S.K.; Poinern, G.E.J. Green Synthesis of Metallic Nanoparticles via Biological Entities. *Materials* **2015**, *8* (11), 7278–7308.
- [26] Dikshit, P.K.; Kumar, J.; Das, A.K.; Sadhu, S.; Sharma, S.; Singh, S.; Gupta, P.K.; Kim, B.S. Green Synthesis of Metallic Nanoparticles: Applications and Limitations. *Catalysts* **2021**, *11* (8), 902.
- [27] Lydia, D.E.; Khusro, A.; Immanuel, P.; Esmail, G.A.; Al-Dhabi, N.A.; Arasu, M.V. Photo-Activated Synthesis and Characterization of Gold Nanoparticles from Punica Granatum L. Seed oil: An Assessment on Antioxidant and Anticancer Properties for Functional Yoghurt Nutraceuticals. *J. Photochem. Photobiol., B* **2020**, *206*, 111868.
- [28] Barabadi, H.; Vahidi, H.; Kamali, K.D.; Hosseini, O.; Mahjoub, M.A.; Rashedi, M.; Shoushtari, F.J.; Saravanan, M. Emerging Theranostic Gold Nanomaterials to Combat Lung Cancer: A Systematic Review. *J. Cluster Sci.* **2020**, *31*, 323–330.
- [29] Barabadi, H.; Vahidi, H.; Kamali, K.D.; Rashedi, M.; Hosseini, O.; Saravanan, M. Emerging Theranostic Gold Nanomaterials to Combat Colorectal Cancer: A Systematic Review. *J. Cluster Sci.* **2020**, *31*, 651–658.
- [30] Saravanan, M.; Barabadi, H.; Vahidi, H.; Webster, T.J.; Medina-Cruz, D.; Mostafavi, E.; Vernet-Crua, A.; Cholula-Diaz, J.L.; Periakaruppan, P. Emerging Theranostic Silver and Gold Nanobiomaterials for Breast Cancer: Present Status and Future Prospects. In Anand, K.; Saravanan, M.; Chandrasekaran, B.; Khanki, S.; Panchu, S.J.; Chen, Q. (Eds.), *Handbook on Nanobiomaterials for Therapeutics and Diagnostic Applications*, Chapter 19, Amsterdam, Netherlands: Elsevier, **2021**, pp. 439–456.
- [31] Saravanan, M.; Vahidi, H.; Medina Cruz, D.; Vernet-Crua, A.; Mostafavi, E.; Stelmach, R.; Webster, T.J.; Mahjoub, M.A.; Rashedi, M.; Barabadi, H. Emerging Antineoplastic Biogenic Gold Nanomaterials for Breast Cancer Therapeutics: A Systematic Review. *Int. J. Nanomedicine* **2020**, *15*, 3577–3595.
- [32] Barabadi, H.; Vahidi, H.; Mahjoub, M.A.; Kosar, Z.; Kamali, K.D.; Ponmurugan, K.; Hosseini, O.; Rashedi, M.; Saravanan, M. Emerging Antineoplastic Gold Nanomaterials for Cervical Cancer Therapeutics: A Systematic Review. *J. Cluster Sci.* **2020**, *31*, 1173–1184.
- [33] Khatua, A.; Prasad, A.; Priyadarshini, E.; Kumar Patel, A.; Naik, A.; Saravanan, M.; Barabadi, H.; Ghosh, I.; Paul, B.; Paulraj, R.; Meena, R. Emerging Antineoplastic Plant-Based Gold Nanoparticle Synthesis: A Mechanistic Exploration of Their Anticancer Activity Toward Cervical Cancer Cells. *J. Cluster Sci.* **2020**, *31*, 1329–1340.
- [34] Mostafavi, E.; Zarepour, A.; Barabadi, H.; Zarrabi, A.; Truong, L.B.; Medina-Cruz, D. Antineoplastic Activity of Biogenic Silver and Gold Nanoparticles to Combat Leukemia: Beginning a New Era in Cancer Theragnostic. *Biotechnology Reports* **2022**, *34*, e00714.
- [35] Paek, H.J.; Lee, Y.J.; Chung, H.E.; Yoo, N.H.; Lee, J.A.; Kim, M.K.; Lee, J.K.; Jeong, J.; Choi, S.J. Modulation of the Pharmacokinetics of Zinc Oxide Nanoparticles and Their Fates in Vivo. *Nanoscale*. **2013**, *5* (23), 11416–11427.
- [36] Vinluan III, R.D.; Zheng, J. Serum Protein Adsorption and Excretion Pathways of Metal Nanoparticles. *Nanomedicine* **2015**, *10* (17), 2781–2794.
- [37] Koushki, K.; Keshavarz Shahbaz, S.; Keshavarz, M.; Bezsonov, E.E.; Sathyapalan, T.; Sahebkar, A. Gold Nanoparticles: Multifaceted Roles in the Management of Autoimmune Disorders. *Biomolecules* **2021**, *11* (9), 1289.
- [38] Sumbayev, V.V.; Yasinska, I.M.; Garcia, C.P.; Gilliland, D.; Lall, G.S.; Gibbs, B.F.; Bonsall, D.R.; Varani, L.; Rossi, F.; Calzolari, L. Gold Nanoparticles Downregulate Interleukin-1 β -Induced Pro-Inflammatory Responses. *Small* **2013**, *9* (3), 472–477.
- [39] Kingston, M.; Pfau, J.C.; Gilmer, J.; Brey, R. Selective Inhibitory Effects of 50-nm Gold Nanoparticles on Mouse Macrophage and Spleen Cells. *J. Immunotoxicol* **2016**, *13* (2), 198–208.
- [40] Singleton, V.L.; Orthofer, R.; Lamuela-Raventós, R.M. Analysis of Total Phenols and Other Oxidation Substrates and Antioxidants by Means of Folin-Ciocalteu Reagent. *Method. Enzymol* **1999**, *299*, 152–178.
- [41] Moldovan, B.; Popa, A.; David, L. Effects of Storage Temperature on the Total Phenolic Content of Cornelian Cherry (*Cornus mas* L.) Fruits Extracts. *J. Appl. Bot. Food Qual* **2016**, *89*, 208–211.
- [42] Winter, C.A.; Riskey, E.A.; Nuss, G.W. Carrageenin-induced Edema in Hind Paw of the Rat as an Assay for Antiinflammatory Drugs. *Proc. Soc. Exp. Biol. Med* **1962**, *111*, 544–547.
- [43] Moldovan, B.; David, L.; Vulcu, A.; Olenic, L.; Perdeschrepler, M.; Fischer-Fodor, E.; Baldea, I.; Clichici, S.; Filip, G.A. *In vitro* and *in vivo* Anti-Inflammatory Properties of Green Synthesized Silver Nanoparticles Using *Viburnum opulus* L. Fruits Extract. *Materials Science and Engineering: C* **2017**, *79*, 720–727.
- [44] David, L.; Moldovan, B.; Baldea, I.; Olteanu, D.; Bolfa, P.; Clichici, S.; Filip, G.A. Modulatory Effects of Cornus Sanguinea L. Mediated Green Synthesized Silver Nanoparticles on Oxidative Stress, COX-2/NOS2 and NFkB/pNFkB Expressions in Experimental Inflammation in Wistar Rats. *Mater Sci Eng C Mater Biol Appl* **2020**, *110*, 110709.

- [45] Noble, J.E.; Bailey, M.J. Chapter 8: Quantitation of Protein. In: Burgess, R.R.; Deutscher, M.P. (Eds.), *Methods in Enzymology*, vol. 463, 2nd ed., San Diego, California, 2009; pp. 73–95.
- [46] Kouadio, F.; Kanko, C.; Juge, M.; Grimaud, N.; Jean, A.; N'Guessan, Y.T.; Petit, J.Y. Analgesic and Antiinflammatory Activities of an Extract from *Parkia biglobosa* Used in Traditional Medicine in the Ivory Coast. *Phytother. Res* **2000**, *14* (8), 635–637.
- [47] Conti, M.; Morand, P.C.; Levillain, P.; Lemonnier, A. Improved Fluorometric Determination of Malonaldehyde. *Clin. Chem* **1991**, *37* (7), 1273–1275.
- [48] Hu, M.L. *Methods Enzymol.* **1994**, *233*, 380–384.
- [49] Pippenger, C.E.; Browne, R.W.; Armstrong, D. Regulatory Antioxidant Enzymes. In: Armstrong, D. (Ed.), *Free Radical and Antioxidant Protocols. Methods in Molecular Biology*, vol. 108, Humana Press Inc.: Totowa, NJ, 1998; pp. 299–313.
- [50] Flohé, L.; Günzler, W.A. Assays of Glutathione Peroxidase. *Methods Enzymol.* **1984**, *105*, 114–121.
- [51] Coura, C.O.; Souza, R.B.; Rodrigues, J.A.G.; de Sousa Oliveira Vanderlei, E.; Fernandes de Araújo, I.W.; Ribeiro, N.A.; Frota, A.F.; Ribeiro, K.A.; Chaves, H.V.; Alves Pereira, K.M.; Silva da Cunha, R.M.; Bezerra, M.M.; Barros Benevides, N.M. Mechanisms Involved in the Anti-Inflammatory Action of a Polysulfated Fraction from *Gracilaria Cornea* in Rats. *PLoS One* **2015**, *10* (3), e0119319.
- [52] Tudor, D.V.; Bâldea, I.; Lupu, M.; Kacso, T.; Kutasi, E.; Hopârtean, A.; Stretea, R.; Filip, A.G. COX-2 as a Potential Biomarker and Therapeutic Target in Melanoma. *Cancer Biol. Med* **2020**, *17* (1), 20–31.
- [53] Moldovan, B.; Ghic, O.; David, L.; Chisbora, C. The Influence of Storage on the Total Phenols Content and Antioxidant Activity of the Cranberrybush (*Viburnum opulus* L.) Fruits Extract. *Rev. Chim. Bucharest* **2012**, *63*, 463–464.
- [54] Bidian, C.; Filip, G.A.; David, L.; Florea, A.; Moldovan, B.; Popa Robu, D.; Olteanu, D.; Radu, T.; Clichici, S.; Mitrea, D.R.; Baldea, I. The Impact of Silver Nanoparticles Phytosynthesized with *Viburnum Opulus* L. Extract on the Ultrastructure and Cell Death in the Testis of Offspring Rats. *Food Chem. Toxicol* **2021**, *150*, 112053.
- [55] Baldea, I.; Florea, A.; Olteanu, D.; Clichici, S.; David, L.; Moldovan, B.; Cenariu, M.; Achim, M.; Suharoschi, R.; Danescu, S.; Vulcu, A.; Filip, G.A. Effects of Silver and Gold Nanoparticles Phytosynthesized with *Cornus mas* Extract on Oral Dysplastic Human Cells. *Nanomedicine* **2020**, *15* (1), 55–75.
- [56] Clichici, S.; David, L.; Moldovan, B.; Baldea, I.; Olteanu, D.; Filip, M.; Nagy, A.; Luca, V.; Crivii, C.; Mircea, P.; Katona, G.; Filip, G.A. Hepatoprotective Effects of Silymarin Coated Gold Nanoparticles in Experimental Cholestasis. *Mater. Sci. Eng. C Mater. Biol. Appl* **2020**, *115*, 111117.
- [57] Unal, I.S.; Demirbas, A.; Onal, I.; Ildiz, N.; Ocsoy, I. One Step Preparation of Stable Gold Nanoparticle Using Red Cabbage Extracts Under UV Light and Its Catalytic Activity. *J. Photochem. Photobiol. B* **2020**, *204*, 111800.
- [58] Irvani, S. Green Synthesis of Metal Nanoparticles Using Plants. *Green Chem.* **2011**, *13* (10), 2638–2650.
- [59] Opris, R.; Toma, V.; Olteanu, D.; Baldea, I.; Baci, A.M.; Imre Lucaci, F.; Berghian-Sevastre, A.; Tatomir, C.; Moldovan, B.; Clichici, S.; David, L.; Florea, A.; Filip, G.A. Effects of Silver Nanoparticles Functionalized with *Cornus mas* L. Extract on Architecture and Apoptosis in rat Testicle. *Nanomedicine* **2019**, *14* (3), 275–299.
- [60] Honary, S.; Gharaei-Fathabad, E.; Barabadi, H.; Naghibi, F. Fungus-Mediated Synthesis of Gold Nanoparticles: A Novel Biological Approach to Nanoparticle Synthesis. *J. Nanosci. Nanotechnol.* **2013**, *13* (2), 1427–1430.
- [61] Barabadi, H.; Najafi, M.; Samadian, H.; Azarnezhad, A.; Vahidi, H.; Mahjoub, M.A.; Koohiyan, M.; Ahmadi, A. A Systematic Review of the Genotoxicity and Antigenotoxicity of Biologically Synthesized Metallic Nanomaterials: Are Green Nanoparticles Safe Enough for Clinical Marketing? *Medicina* **2019**, *55* (8), 439.
- [62] Ghomi, A.R.G.; Mohammadi-Khanaposhti, M.; Vahidi, H.; Kobarfard, F.; Reza, M.A.S.; Barabadi, H. Fungus-mediated Extracellular Biosynthesis and Characterization of Zirconium Nanoparticles Using Standard *Penicillium* Species and Their Preliminary Bactericidal Potential: A Novel Biological Approach to Nanoparticle Synthesis. *Iran. J. Pharm. Res.* **2019**, *18* (4), 2101–2110.
- [63] Honary, S.; Barabadi, H.; Ebrahimi, P.; Naghibi, F.; Alizadeh, A. Development and Optimization of Biometal Nanoparticles by Using Mathematical Methodology: A Microbial Approach. *J. Nano Res.* **2015**, *30*, 106–115.
- [64] Mansouri, M.T.; Hemmati, A.A.; Naghizadeh, B.; Mard, S.A.; Rezaie, A.; Ghorbanzadeh, B. A Study of the Mechanisms Underlying the Anti-Inflammatory Effect of Ellagic Acid in Carrageenan-Induced Paw Edema in Rats. *Indian J. Pharmacol* **2015**, *47* (3), 292–298.
- [65] Khedir, S.B.; Mzid, M.; Bardaa, S.; Moalla, D.; Sahnoun, Z.; Rebai, T. In Vivo Evaluation of the Anti-Inflammatory Effect of *Pistacia lentiscus* Fruit Oil and Its Effects on Oxidative Stress. *Evid. Based Complement. Alternat. Med* **2016**, *2016*, 6108203.
- [66] Eken, A.; Yücel, O.; Boşgelmez, I.I.; Baldemir, A.; Çubuk, S.; Cermik, A.H.; Ünlü Endirlik, B.; Bakir, E.; Yildizhan, A.; Güler, A.; Koşar, M. An Investigation on Protective Effect of *Viburnum opulus* L. Fruit Extract Against Ischemia/Reperfusion-Induced Oxidative Stress After Lung Transplantation in Rats. *Kafkas Univ. Vet. Fak. Derg* **2017**, *23* (3), 437–444.
- [67] Altun, M.L.; Çitoğlu, G.S.; Yilmaz, B.S.; Özbek, H. Antinociceptive and Anti-Inflammatory Activities of *Viburnum opulus*. *Pharm. Biol* **2009**, *47* (7), 653–658.
- [68] Guyton and Hall. *Textbook of Medical Physiology*, 13th ed.; Elsevier Inc: Philadelphia, 2016.
- [69] Jeon, K.I.; Byun, M.S.; Jue, D.M. Gold Compound Auranofin Inhibits IκappaB Kinase (IKK) by Modifying Cys-179 of IKKbeta Subunit. *Exp. Mol. Med* **2003**, *35* (2), 61–66.
- [70] Ma, J.S.; Kim, W.J.; Kim, J.J.; Kim, T.J.; Ye, S.K.; Song, M.D.; Kang, H.; Kim, D.W.; Moon, W.K.; Lee, K.H. Gold Nanoparticles Attenuate LPS-Induced NO Production Through the Inhibition of NF-KappaB and IFN-Beta/STAT1 Pathways in RAW264.7 Cells. *Nitric Oxide* **2010**, *23* (3), 214–219.
- [71] Lai, T.H.; Chung, C.H.; Chen, B.H.; Hung, C.F.; Inbaraj, B.S.; Ma, M.C.; Chen, H.M.; Tsou, C.J.; Wu, P.H.; Wu, W.B. Gold Nanoparticles Compromise TNF-α-Induced Endothelial Cell Adhesion Molecule Expression Through NF-κB and Protein Degradation Pathways and Reduce Neointima Formation in a Rat Carotid Balloon Injury Model. *J. Biomed. Nanotechnol* **2016**, *12*, 2185–2201.

- [72] Rizwan, H.; Mohanta, J.; Si, S.; Pal, A. Gold Nanoparticles Reduce High Glucose-Induced Oxidative-Nitrosative Stress Regulated Inflammation and Apoptosis via Tuberin-mTOR/NF-kB Pathways in Macrophages. *Int. J. Nanomed* **2017**, *12*, 5841–5862.
- [73] Khan, M.A.; Khan, M.J. Nano-gold Displayed Anti-Inflammatory Property via NF-kB Pathways by Suppressing COX-2 Activity. *Artif. Cells Nanomed. Biotechnol* **2018**, *46*, 1149–1158.
- [74] Dohnert, M.B.; Ferreira, G.K.; Silveira, P.C.L.; Zanoni, E.T.; Dohnert, L.H.; de Souza, C.T.; Paula, M.M.S. Inflammatory Cytokines Content in Achilles Tendinopathy After Phonophoresis Treatment Combined with Gold Nanoparticles and Diclophenac Diethylammonium in Rats. *Inflammation* **2015**, *38* (3), 1044–1049.
- [75] Sabat, R.; Grütz, G.; Warszawska, K.; Kirsch, S.; Witte, E.; Wolk, K.; Geginat, J. Biology of Interleukin-10. *Cytokine Growth Factor Rev.* **2010**, *21* (5), 331–344.
- [76] Martire-Greco, D.; Rodriguez-Rodrigues, N.; Landoni, V.I.; Rearte, B.; Isturiz, M.A.; Fernández, G.C. Interleukin-10 Controls Human Peripheral PMN Activation Triggered by Lipopolysaccharide. *Cytokine* **2013**, *62* (3), 426–432.
- [77] Mortezaee, K.; Najafi, M.; Samadian, H.; Barabadi, H.; Azarnezhad, A.; Ahmadi, A. Redox Interactions and Genotoxicity of Metal-Based Nanoparticles: A Comprehensive Review. *Chem.-Biol. Interact.* **2019**, *312*, 108814.